

Advancing Block Diffusion Language Models for Test-Time Scaling

Yi Lu ^{*1} Deyang Kong ^{*2} Jianing Wang ³ Linsen Guo ³ Xue Wang ³ Qi Guo ² Tao Gui ¹ Xuanjing Huang ¹
Wei Ye ² Shikun Zhang ² Wei Wang ³

Abstract

Recent advances in block diffusion language models have demonstrated competitive performance and strong scalability on reasoning tasks. However, existing BDLMs have limited exploration under the test-time scaling setting and face more severe decoding challenges in long Chain-of-Thought reasoning, particularly in balancing the decoding speed and effectiveness. In this work, we propose a unified framework for test-time scaling in BDLMs that introduces adaptivity in both decoding and block-wise generation. At the decoding level, we propose Bounded Adaptive Confidence Decoding (BACD), a difficulty-aware sampling strategy that dynamically adjusts denoising based on model confidence, accelerating inference while controlling error accumulation. Beyond step-wise adaptivity, we introduce Think Coarse, Critic Fine (TCCF), a test-time scaling paradigm that allocates large block sizes to exploratory reasoning and smaller block sizes to refinement, achieving an effective efficiency-effectiveness balance. To enable efficient and effective decoding with a large block size, we adopt Progressive Block Size Extension, which mitigates performance degradation when scaling block sizes. Extensive experiments show that applying BACD and TCCF to TDAR-8B yields significant improvements over strong baselines such as TraDo-8B (2.26 \times speedup, +11.2 points on AIME24). These results mark an important step toward unlocking the potential of BDLMs for test-time scaling in complex reasoning tasks. Our code and models are available at <https://github.com/LuLuLuyi/TDAR>.

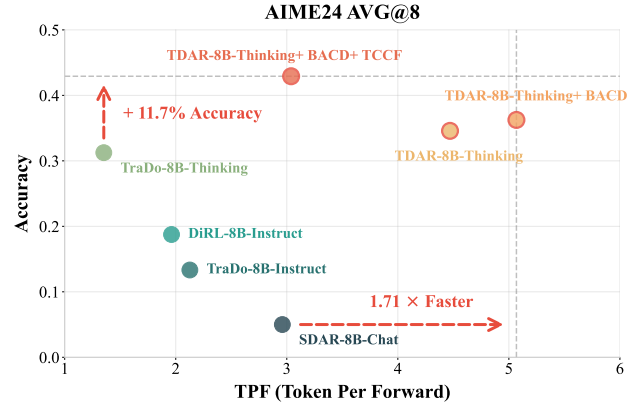


Figure 1. Performance and speed comparison of BDLMs. Our TDAR-8B-Thinking achieves 1.71 \times speedup with BACD and +11.7% accuracy with TCCF compared to the best baselines.

1. Introduction

Recent advances in Large Diffusion Language Models (dLLMs), exemplified by LLaDA (Nie et al., 2025), Dream (Ye et al., 2025b), Gemini Diffusion (Gemini, 2025), have demonstrated the scalability of this paradigm (Nie et al., 2024; Gong et al., 2025a) and have achieved remarkable performance on mathematics (Ye et al., 2025b; Cheng et al., 2025), code generation (Gong et al., 2025b; Wang et al., 2025), and general reasoning tasks (Ye et al., 2025a; Shao et al., 2025). Building on the recent success of dLLMs, Block Diffusion Language Models (BDLMs) (Arriola et al., 2025) have emerged as a promising direction that integrates diffusion with traditional autoregressive (AR) decoding, enabling efficient KV caching and substantially improving inference efficiency and generation flexibility.

However, existing BDLMs (Bie et al., 2025; Wang et al., 2025; Zhu et al., 2025c) primarily focus on simple reasoning tasks and offer limited exploration under the test-time scaling paradigm. While Wang et al. (2025) train a block diffusion model for complex reasoning, they do not systematically investigate how block diffusion should balance efficiency and effectiveness in such settings. Test-time scaling with long Chain-of-Thought (CoT) reasoning presents a double-edged scenario for block diffusion, i.e., although it naturally favors parallel decoding, the increased reasoning complexity substantially intensifies the trade-off between

^{*}Equal contribution ¹Fudan University ²Peking University ³Meituan LongCat Team. Correspondence to: Tao Gui <tgui@fudan.edu.cn>, Wei Ye <wye@pku.edu.cn>, Wei Wang <wangwei432@meituan.com>.

efficiency and effectiveness. In Figure 1, we observe that current BDLMs struggle to simultaneously achieve high performance and efficiency on complex reasoning tasks, where improvements in efficiency often lead to a substantial degradation in performance.

To address the efficiency–effectiveness trade-off of block diffusion under test-time scaling, we propose a unified framework that introduces adaptivity in both decoding and generation strategies. Our key insight is that long reasoning trajectories are inherently heterogeneous: different parts vary not only in local sampling difficulty, but also in their role within the overall reasoning process. Effectively exploiting this non-uniformity is crucial for achieving both efficiency and reliability in block diffusion. At the decoding stage, we introduce **Bounded Adaptive Confidence Decoding (BACD)**, a dynamic sampling strategy that adapts the denoising process to the varying difficulty of long reasoning trajectories. Using the average confidence of previously decoded tokens as a difficulty signal, our method enables aggressive acceleration when the model is highly confident via an upper-bound threshold, while enforcing a lower-bound threshold to prevent excessive error accumulation under uncertainty. Beyond step-wise decoding adaptivity, we propose **Think Coarse, Critic Fine (TCCF)**, a test-time scaling paradigm that exploits the heterogeneous roles within long reasoning trajectories. While exploratory reasoning can be generated efficiently with coarse-grained decoding, refinement and summarization demand finer granularity to ensure correctness. TCCF therefore allocates larger block sizes to exploratory segments and smaller block sizes to refinement-oriented segments, enabling an effective balance between efficiency and reasoning quality under test-time scaling. To enable efficient and effective decoding in a large block size, we adopt Progressive Block Size Extension, a multi-stage denoising fine-tuning strategy, which mitigates performance degradation when scaling block sizes. These designs enable BDLMs to effectively balance efficiency and reasoning quality, unlocking their potential for test-time scaling on complex reasoning tasks.

To evaluate the effectiveness and generalizability of our approach, we conduct extensive experiments on a diverse set of six reasoning benchmarks, including mathematics, code generation, and STEM. Results show that TDAR-8B-Thinking with BACD achieves state-of-the-art performance among 8B-scale block diffusion language models, while providing up to $3.37\times$ speedup over standard autoregressive decoding. In addition, the TCCF paradigm further improves reasoning performance and offers a better trade-off between speed and accuracy. In summary, our contributions are threefold:

- We propose Bounded Adaptive Confidence Decoding, a difficulty-aware decoding strategy that dynamically

adapts denoising at test time, improving both performance and efficiency with strong robustness.

- We introduce Think Coarse, Critic Fine, a new test-time scaling paradigm that combines coarse-grained exploration with fine-grained refinement, significantly enhancing complex reasoning performance with minimal efficiency overhead.
- We identify large block sizes as a key factor for BDLM acceleration and propose Progressive Block Size Extension, which mitigates performance degradation when scaling block sizes and unlocks the acceleration potential of BDLMs.

2. Preliminary

2.1. Block Diffusion Language Models

Block Diffusion Language Models (Arriola et al., 2025; Wu et al., 2025b; Cheng et al., 2025) interpolate between autoregressive and diffusion paradigms. A token sequence \mathbf{x} is partitioned into K non-overlapping blocks $\mathbf{x} = (\mathbf{x}^1, \dots, \mathbf{x}^K)$, where the block size of \mathbf{x}^k represents as B . The model factorizes the likelihood autoregressively over blocks:

$$\log p_\theta(\mathbf{x}) = \sum_{k=1}^K \log p_\theta(\mathbf{x}^k \mid \mathbf{x}^{<k}), \quad (1)$$

where $\mathbf{x}^{<k}$ denotes the preceding clean blocks. Each conditional distribution $p_\theta(\mathbf{x}^k \mid \mathbf{x}^{<k})$ is modeled via a discrete masked diffusion process: a forward process and a reverse process. The forward process $q(\mathbf{x}_t^k \mid \mathbf{x}_0^k)$ gradually masks tokens within block \mathbf{x}^k . When adopt a linear noise schedule defined by $\alpha_t = 1 - t$ at time $t \in [0, 1]$, each token is independently replaced by a special [MASK] token \mathbf{m} with probability $1 - \alpha_t$:

$$q(\mathbf{x}_t^k \mid \mathbf{x}_0^k) = \prod_{i=1}^B \text{Cat}((\mathbf{x}_t^k)_i; (1-t)(\mathbf{x}_0^k)_i + t\mathbf{m}). \quad (2)$$

The reverse process reconstructs the original block \mathbf{x}_0^k from the noisy state \mathbf{x}_t^k given the history $\mathbf{x}^{<k}$. The model predicts the distribution of original tokens in parallel:

$$p_\theta(\mathbf{x}_0^k \mid \mathbf{x}_t^k, \mathbf{x}^{<k}) = \prod_{i=1}^B p_\theta((\mathbf{x}_0^k)_i \mid \mathbf{x}_t^k, \mathbf{x}^{<k}). \quad (3)$$

Standard block discrete denoising diffusion models minimize the Negative Evidence Lower Bound (NELBO). Under the linear noise schedule $\alpha_t = 1 - t$, the objective is scaled by the inverse noise level $1/t$. The loss is computed exclusively on the set of masked positions \mathcal{M}_t^k within each block:

$$\mathcal{L}(\theta) = \mathbb{E}_{t, \mathbf{x}} \left[-\frac{1}{t} \sum_{k=1}^K \sum_{i \in \mathcal{M}_t^k} \log p_\theta((\mathbf{x}_0^k)_i \mid \mathbf{x}_t^k, \mathbf{x}^{<k}) \right] \quad (4)$$

2.2. Sampling Algorithm for BDLMs

Generation in BDLMs proceeds block-by-block. For the k -th block \mathbf{x}^k , decoding starts from a fully masked state \mathbf{x}_T^k . At each denoising step t , the model predicts token probabilities for all masked positions $i \in \mathcal{M}_t^k$ conditioned on the current state \mathbf{x}_t^k , history $\mathbf{x}^{<k}$, and prompt \mathbf{p} . We define the *confidence* score for position i as:

$$c_i(\mathbf{x}_t^k) := \max_{v \in \mathcal{V}} p_\theta((\mathbf{x}_0^k)_i = v \mid \mathbf{x}_t^k, \mathbf{x}^{<k}, \mathbf{p}). \quad (5)$$

A subset of masked tokens $\mathcal{D}_t \subseteq \mathcal{M}_t^k$ is then selected for unmasking based on c_i . We introduce two widely used strategies for BDLMs:

Static Confidence Decoding. (Nie et al., 2025) A fixed number of tokens, $n = \lceil B/N \rceil$, are decoded at each step, where N is the total denoising steps. Specifically, \mathcal{D}_t consists of the n masked positions with the highest confidence scores.

Dynamic Confidence Decoding. (Wu et al., 2025d) Tokens are decoded adaptively based on a confidence threshold τ . The selection set is defined as $\mathcal{D}_t = \{i \in \mathcal{M}_t^k \mid c_i(\mathbf{x}_t^k) > \tau\}$. This strategy accelerates inference by rapidly decoding easy tokens.

3. Method

We propose a unified framework for test-time scaling in Block Diffusion Language Models (BDLMs), which exploits the non-uniform nature of long reasoning trajectories through adaptivity at two levels. At the decoding level, we design a dynamic sampling strategy that adjusts denoising steps to local difficulty. At the reasoning-phase level, we introduce a new test-time scaling paradigm that adapts block sizes to different stages of reasoning. An overview of our framework is shown in Figure 2.

3.1. Bounded Adaptive Confidence Decoding

Dynamic decoding for block diffusion models typically relies on a fixed confidence threshold, which becomes increasingly brittle as block size grows: high thresholds lead to inefficient decoding, while low thresholds cause error accumulation due to overly aggressive unmasking. To address this issue, we propose **Bounded Adaptive Confidence Decoding (BACD)**, a dynamic decoding strategy that adaptively adjusts the unmasking threshold while enforcing explicit upper and lower bounds. The detailed decoding procedure is summarized in Algorithm 1.

BACD maintains a list of confidence scores from previously decoded tokens and uses their average to guide future decoding decisions. Let \mathbf{c}_{t-1} denote the list of confidence scores

collected before step t . In the initial state where \mathbf{c}_{t-1} is empty, we set $\tau_t = \tau_h$. At each decoding step, we compute the average confidence $\bar{c}_{t-1} = \text{mean}(\mathbf{c}_{t-1})$. To stabilize decoding behavior, we introduce two thresholds: an upper bound τ_h and a lower bound τ_l . The effective decoding threshold τ_t is determined via a clipping operation:

$$\tau_t = \text{clip}(\bar{c}_{t-1}, \tau_l, \tau_h). \quad (6)$$

Using τ_t , we select the set of tokens to be unmasked at step t :

$$\mathcal{D}_t = \{i \in \mathcal{M}_t^k \mid c_i(\mathbf{x}_t^k) > \tau_t\}. \quad (7)$$

To guarantee convergence, if $\mathcal{D}_t = \emptyset$, we unmask the token with the highest confidence score. The confidence scores of newly decoded tokens are then appended to the list \mathbf{c} for subsequent steps. By bounding the adaptive threshold, BACD prevents overly conservative or overly aggressive decoding, enabling a more stable trade-off between efficiency and generation quality.

Algorithm 1: Bounded Adaptive Confidence Decoding

Input: Masked block \mathbf{x}_T^k , bounds τ_h, τ_l
Output: Clean block \mathbf{x}_0^k
 Initialize confidence list $\mathbf{c} \leftarrow []$;
while masked tokens exist in \mathbf{x}^k **do**
 Let $\mathcal{M} \leftarrow \{i \mid (\mathbf{x}^k)_i = [\text{MASK}]\}$;
 Compute confidence scores c_i for all $i \in \mathcal{M}$;
 Calculate mean $\bar{c} \leftarrow \text{mean}(\mathbf{c})$ if $\mathbf{c} \neq []$ else τ_h ;
 Set threshold $\tau \leftarrow \text{clip}(\bar{c}, \tau_l, \tau_h)$;
 Select candidates $\mathcal{D} \leftarrow \{i \in \mathcal{M} \mid c_i > \tau\}$;
if $\mathcal{D} = \emptyset$ **then** $\mathcal{D} \leftarrow \{\arg \max_{i \in \mathcal{M}} c_i\}$;
 Unmask tokens at indices \mathcal{D} and append scores to \mathbf{c} ;

3.2. Think Coarse, Critic Fine

Long CoT reasoning is not uniform across its trajectory. Different segments of a reasoning process serve distinct functional roles. In particular, early segments often focus on exploratory reasoning, while later segments emphasize refinement, verification, and summarization. However, block diffusion models exhibit a clear trade-off between block size and generation quality: larger block sizes enable faster decoding but may degrade accuracy, whereas smaller block sizes improve precision at the cost of efficiency. As a result, a single block size is insufficient to balance efficiency and reasoning quality across all stages.

Motivated by this observation, we propose **Think Coarse, Critic Fine (TCCF)**, a test-time scaling paradigm that adapts the block size to different stages of reasoning. TCCF leverages the trade-off between block size and generation quality in block diffusion, allocating computation according to the functional role of each reasoning segment. Given

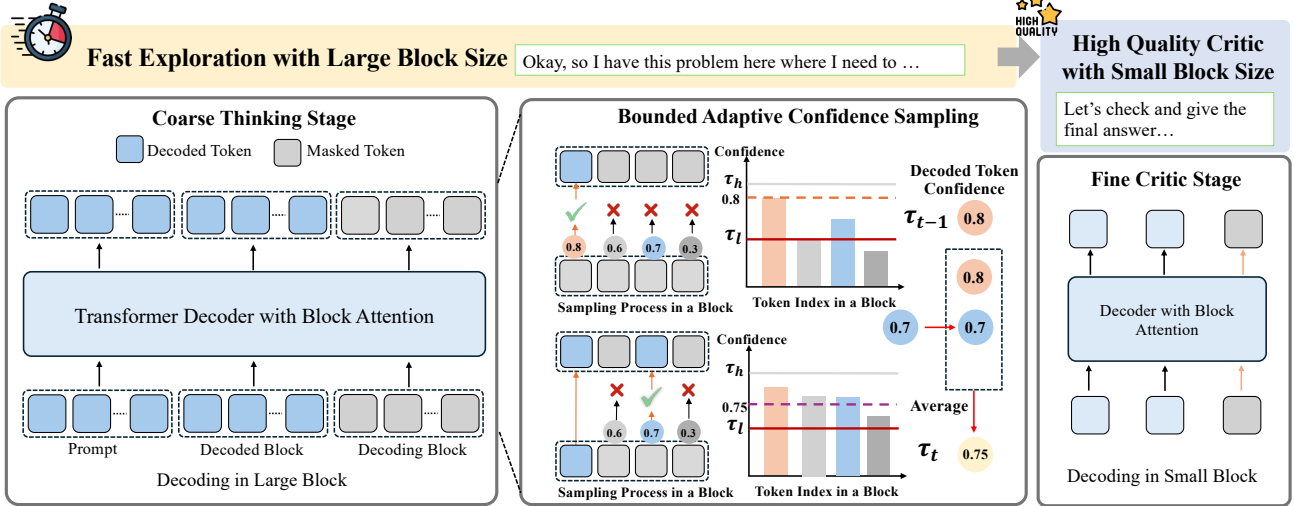


Figure 2. Overview of our reasoning process. We use Bounded Adaptive Confidence Decoding to enable fast exploration with large block sizes, and apply small block sizes for fine-grained refinement.

an input prompt \mathbf{p} , TCCF decomposes inference into two stages:

Coarse Thinking. The model first generates an exploratory reasoning trajectory \mathbf{r} using a large block size B_{think} to maximize generation efficiency:

$$\mathbf{r} \sim p_{\theta}(\cdot \mid \mathbf{p}; B_{\text{think}}). \quad (8)$$

Fine Critic. Conditioned on \mathbf{p} and the exploratory trajectory \mathbf{r} , the model performs refinement and consolidation using a smaller block size $B_{\text{critic}} < B_{\text{think}}$ to improve reasoning reliability:

$$\mathbf{y} \sim p_{\theta}(\cdot \mid \mathbf{p}, \mathbf{r}; B_{\text{critic}}). \quad (9)$$

Training with Large Block Sizes. TCCF relies on large block sizes during coarse thinking, which can lead to performance degradation if the model is trained with a fixed small block size. To enable stable training under large block sizes, we adopt **Progressive Block Size Extension**, a multi-stage supervised fine-tuning strategy that gradually increases the block size. Given a training instance (\mathbf{p}, \mathbf{x}) consisting of an instruction prompt \mathbf{p} and a target response \mathbf{x} , the supervised fine-tuning objective is:

$$\mathcal{L}_{\text{SFT}}(\theta) = \mathbb{E}_{t,(\mathbf{e},\mathbf{x})} \left[-\frac{1}{t} \sum_{k=1}^K \sum_{i \in \mathcal{M}_t^k} \log p_{\theta}((\mathbf{x}_0^k)_i \mid \mathbf{x}_t^k, \mathbf{x}^{<k}, \mathbf{p}) \right]. \quad (10)$$

By progressively increasing the block size during fine-tuning, this strategy mitigates performance degradation when scaling block sizes, which is crucial for enabling the coarse thinking stage in TCCF.

4. Experiment

4.1. Experiment Setup

Adaptation to Long CoT Reasoning BDLMs. We adapt Qwen3-8B-base into Block DLMs following Cheng et al. (2025). We first train with a blockwise diffusion objective ($B = 4$) on a 50B-token annealing corpus, then perform SFT on long CoT data with progressive block-size expansion from $B = 4$ to $B = 64$. Based on the performance-efficiency trade-off analysis in Section 5.2, we select the model trained with a block size of $B = 16$ as our 8B reasoning model denoted as **TDAR-8B-thinking**. We also train an autoregressive model from Qwen3-8B-base using the same recipe. We compare the base model Qwen3-8B-base[†] in Appendix A. Implementation details are provided in Appendix B.1.

Datasets and Baselines. To comprehensively evaluate the reasoning capabilities of BDLMs, we select representative benchmarks covering three categories: mathematical reasoning, code generation, and STEM reasoning. Specifically, the mathematical datasets include Math500 (Hendrycks et al., 2021), AIME2024 (MAA, 2024), AIME2025 (MAA, 2025), and AMC2023 (AMC, 2023). For code generation, we use LiveCodeBench (v5)¹ (Jain et al., 2024). STEM reasoning is evaluated using GPQA-diamond (Rein et al., 2023).

We compare our method against state-of-the-art open-source BDLMs, including Fast-dllm-v2 (Wu et al., 2025a), SDAR-8B-Chat (Cheng et al., 2025), DiRL-8B-Instruct (Zhu et al., 2025c), TraDo-8B-Instruct (Wang et al., 2025), and TraDo-8B-Thinking (Wang et al., 2025). To compare with masked

¹The time range spans from August 2024 to May 2025.

Table 1. Performance comparison of various models on six reasoning benchmarks. \dagger indicates that the models are derived from the Qwen3 Base models by performing the identical CPT and SFT.

Method	Math500		AIME24		AIME25		AMC23		LCB		GPQA		AVG	
	TPF	ACC	TPF	AVG@8	TPF	AVG@8	TPF	AVG@8	TPF	ACC	TPF	ACC	TPF	ACC
<i>Autoregressive Language Model</i>														
Qwen3-8B-Thinking \dagger	1.00	88.2	1.00	63.3	1.00	55.8	1.00	88.8	1.00	59.5	1.00	49.0	1.00	67.4
<i>Masked Diffusion Language Model</i>														
LLaDA	3.91	41.2	3.44	6.7	3.66	0.0	4.07	12.5	2.83	4.7	3.14	17.2	3.51	13.7
LLaDA-1.5	3.97	42.2	3.34	0.0	3.68	0.0	4.01	10.0	2.86	4.3	3.01	24.2	3.48	13.5
LLaDA-MoE	2.70	56.6	2.89	3.3	2.71	0.0	3.16	32.5	2.05	12.9	2.18	27.8	2.62	22.2
<i>Block Diffusion Language Model</i>														
Fast-dLLM-v2	2.81	59.4	2.58	0.0	2.58	0.0	2.77	25.0	1.73	6.8	2.09	28.3	2.43	19.9
SDAR-8B-Chat	2.21	52.6	2.96	5.0	2.35	7.1	2.83	22.5	1.60	7.5	1.32	10.6	2.21	17.6
DiRL-8B-Instruct	2.30	78.2	1.96	18.8	1.92	15.8	2.05	65.6	2.64	10.4	2.27	44.4	2.19	38.9
TraDo-8B-Instruct	2.36	75.0	2.13	13.3	2.00	12.5	2.23	55.3	1.42	7.2	1.43	27.3	1.93	31.8
TraDo-8B-Thinking	1.28	84.0	1.35	31.3	1.35	26.3	1.37	72.8	1.10	22.6	1.16	46.0	1.27	47.1
+ BACD	1.33	85.0	1.44	32.9	1.44	27.5	1.45	73.8	1.15	23.3	1.18	49.5	1.33	48.7
+ BACD +TCCF	1.28	85.6	1.36	35.8	1.33	27.1	1.36	74.1	1.11	21.9	1.14	49.5	1.27	49.0
TDAR-8B-thinking (ours)	1.62	81.6	4.47	34.6	4.17	30.8	5.03	69.1	1.25	40.5	1.28	46.5	2.97	50.5
+ BACD	1.88	83.4	5.07	36.3	4.73	30.4	5.59	71.3	1.46	40.1	1.49	46.0	3.37	51.2
+ BACD +TCCF	1.75	84.0	3.04	42.9	2.79	35.8	2.68	80.0	1.32	42.6	1.39	50.0	2.16	55.9

diffusion language models, we involve LLaDA (Nie et al., 2025), LLaDA-1.5 (Zhu et al., 2025a), LLaDA-MoE (Zhu et al., 2025b). We also involve an autoregressive model derived from the same base model by performing the identical CPT and SFT (denoted as Qwen3-8B-Thinking \dagger).

Evaluation Setup We adopt the optimal block size B recommended in their official repositories: $B = 4$ for SDAR-8B-Chat, DiRL-8B-Instruct, and TraDo-8B; $B = 32$ for Fast-dLLM-v2. For our TDAR-8B-thinking, we set $B = 16$. For decoding algorithms, we adapt widely used algorithms from dLLMs: Dynamic Confidence-Aware Decoding (Wu et al., 2025c). We employ Dynamic Confidence Decoding with a threshold $\tau = 0.9$ as the default algorithm for main results. For BACD, we set the upper bound τ_u to 0.9 and the lower bound τ_l to 0.6. Evaluation details are shown in Appendix B.2. For the TCCF paradigm, we configure TDAR-8B-thinking with $B_{\text{think}} = 16$ for Stage 1 and $B_{\text{critic}} = 1$ for Stage 2. Detailed implementation of TCCF paradigm are provided in the Appendix C.

Evaluation Metrics of Efficiency. We evaluate computational efficiency using Effective Tokens Per Forward Pass (TPF). TPF measures the average number of tokens generated per forward pass:

$$\text{TPF} = \frac{\text{Total Generated Tokens}}{\text{Total Forward Passes}}$$

Higher TPF values indicate greater algorithmic speedup. We also conduct throughput analysis measuring tokens per second (TPS) across different batch sizes in Appendix D.

4.2. Main Results

Performance and Speed As shown in Table 1, TDAR-8B-Thinking achieves competitive performance and decoding speed across a wide range of benchmarks. Notably, TDAR-8B-Thinking outperforms the previously best TraDo-8B-Thinking by an average of 3.4 points, while improving the decoding speed from 1.27 tokens per forward pass (TPF) to 2.97 TPF. When combined with the BACD decoding algorithm, TDAR-8B-Thinking achieves further improvements in decoding speed and performance. In particular, the decoding speed of TDAR-8B-Thinking increases from 2.97 TPF to 3.37 TPF, accompanied by an additional performance gain of 1.6 points. The TCCF test-time scaling paradigm further enhances reasoning performance. With TCCF, TDAR-8B-Thinking improves its AIME24 score from 36.3 to 42.9, while still maintaining 3.04 TPF, achieving a strong trade-off between speed and performance.

Generalization of BACD and TCCF We observe that TraDo-8B-Thinking also benefits substantially from BACD decoding, with its average performance improving from 47.1 to 48.7, while achieving higher decoding efficiency. When equipped with the TCCF paradigm, TraDo-8B-Thinking obtains additional performance gains, improving from 48.7 to 49.0, demonstrating that both BACD and TCCF can be broadly applied to different BDLMs. Moreover, we find that BACD and TCCF consistently yield performance improvements across diverse tasks, and the improvements are more significant on complex reasoning benchmarks with longer generation lengths, such as AIME24.

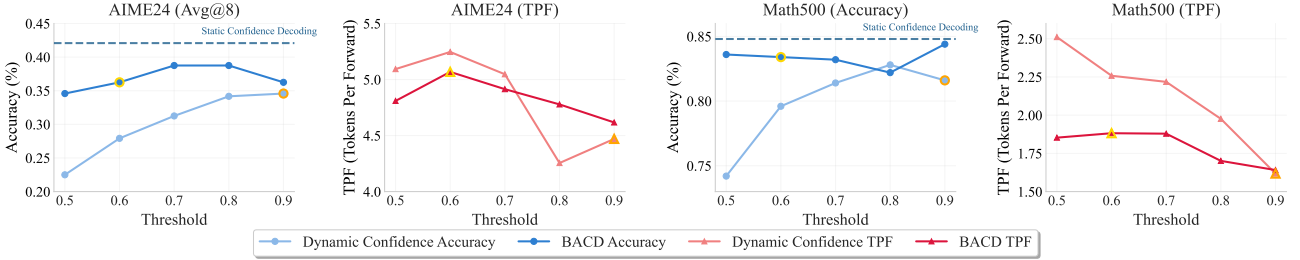


Figure 3. Accuracy and Speed under different thresholds on AIME24 and Math500. Gold marker indicates our selected checkpoint.

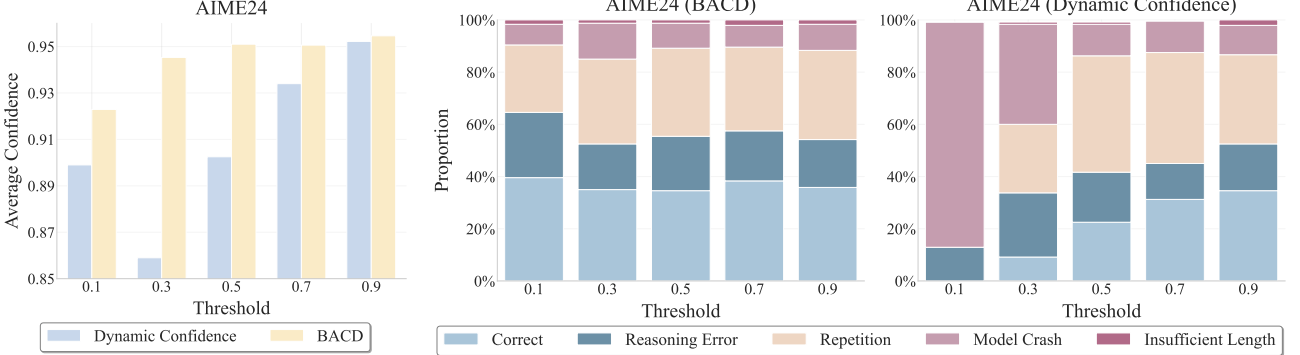


Figure 4. Average token confidence under different confidence thresholds.

Figure 5. Error type analysis under different confidence thresholds for BACD and Dynamic Confidence.

Impact of Block Size TDAR-8B-Thinking adopts a block size of $B = 16$, which significantly outperforms other BDLMs in terms of decoding speed while also achieving superior performance. In contrast, TraDo-8B-Thinking uses a smaller block size ($B = 4$). Although BACD can still improve performance, its average decoding speed only increases marginally from 1.27 to 1.33 TPF. The smaller block size limits the effectiveness of these strategies by reducing decoding flexibility. These results indicate that block size plays a critical role in the speed-performance trade-off.

5. Analysis

5.1. Analysis on Sampling Algorithm

We compare BACD with mainstream sampling algorithms commonly used in BDLMs, including Static Confidence Decoding (Nie et al., 2025) and Dynamic Confidence Decoding (Wu et al., 2025c). For Static Confidence Decoding, we set the denoising step N equal to the block size B . For Dynamic Confidence Decoding, we vary the confidence threshold τ ; for BACD, since the lower confidence bound is the primary factor determining decoding quality, we fix the upper bound τ_h to 0.9 and vary only the lower threshold τ_l .

Performance and Speed under Different Thresholds.

We compare the resulting speed-performance trade-offs in Figure 3. As the threshold decreases, the performance of Dy-

namic Confidence Decoding degrades noticeably, whereas BACD maintains stable performance while achieving consistent efficiency gains. We further compare BACD with sampling algorithms designed for dLLMs, such as Entropy Bounded Decoding (Ben-Hamu et al., 2025) in Appendix E. However, we find that decoding algorithms for dLLMs are typically designed for much larger block sizes, and thus fail to provide acceleration when applied to BDLMs.

Confidence Dynamics Under Different Thresholds. We examine the average confidence of all decoded tokens under different confidence thresholds. As shown in Figure 4, across all thresholds, BACD consistently exhibits a higher average token confidence than the Dynamic Confidence Decoding. The improvement stems from BACD’s lower bound, which acts as a safety guard by preventing transitions into highly uncertain states that could destabilize generation.

Error Types Analysis under Different Thresholds. To further characterize the qualitative differences induced by confidence thresholds, we analyze the distribution of response types under different threshold settings ($\tau \in \{0.1, 0.3, 0.5, 0.7, 0.9\}$). The responses are categorized into five types: correct solutions, reasoning error, repetitive outputs, model crash, and insufficient length. Figure 5 illustrates the statistics of these response types across different thresholds for both BACD and Dynamic Confidence Decoding. As the threshold decreases, Dynamic Confidence

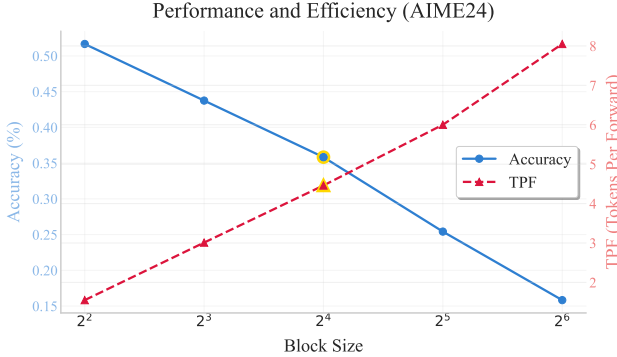


Figure 6. Impact of block size on 8B model performance and efficiency. Gold marker indicates our selected checkpoint.

Decoding shows a sharp increase in pathological failure modes (repetition, crashes), while BACD maintains a relatively stable distribution of response types. This stability explains why BACD preserves generation accuracy across varying threshold settings.

5.2. Analysis on Block Size Extension

Larger block sizes offer significant potential for faster inference and acceleration; however, they inevitably incur a penalty in generation performance. Figure 6 illustrates this trade-off between performance and efficiency across checkpoints trained with varying block sizes. To achieve an optimal balance between generation quality and decoding speed, we select the checkpoint with a block size of 16 for the 8B model as our final configurations.

5.3. Analysis on Think Coarse Critic Fine paradigm

We analyze the effectiveness of the TCCF paradigm under both Dynamic Confidence Decoding and BACD in Figure 7. We observe that TCCF consistently improves performance across different sampling algorithms. For Dynamic Confidence Decoding, as the confidence threshold increases, the quality of the generated text improves, and the performance gains brought by TCCF become increasingly significant. For BACD, we control the lower bound of decoding quality by adjusting τ_l , and find that TCCF yields stable performance improvements across a wide range of thresholds. To illustrate the improvements of TCCF, we provide a detailed case study in Appendix F, showing how the fine critic stage successfully identifies and rectifies errors overlooked during coarse thinking.

6. Ablation Study

6.1. Ablation on BACD Sampling Algorithm

We conduct an ablation study on the design of BACD. We ablate the choices of τ_h and τ_l in Table 2. As shown in

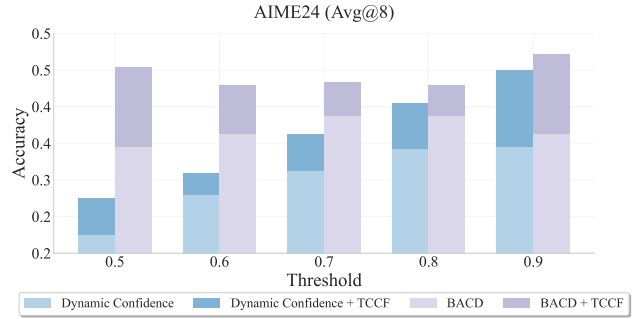


Figure 7. Impact of TCCF strategy on different decoding algorithms.

the table, the lower bound τ_l effectively prevents overly aggressive decoding by suppressing erroneous reasoning trajectories, thereby ensuring a stable performance lower bound. In contrast, the upper bound τ_h enables BACD to exploit higher confidence regions during decoding, providing greater acceleration potential when the model is sufficiently confident.

Table 2. Ablation study on bound strategies for BACD

Method	Math500		GPQA	
	TPF	Acc	TPF	Acc
TDAR-8B-thinking + BACD	1.88	83.4	1.46	45.5
w/o upper bound	1.61	83.6	1.39	43.4
w/o lower bound	2.78	77.2	4.46	27.3
w/o bound	1.76	79.2	1.79	28.8

6.2. Ablation on Progressive Block Size Extension

We conduct an ablation study to evaluate the effectiveness of our progressive block-size expansion strategy compared to directly training with a large fixed block size. We train two variants of the TDAR-8B-Base model with a target block size of $B = 16$ for an equivalent number of tokens. As shown in Table 3, the progressive strategy yields superior results, suggesting that it effectively mitigates the optimization difficulties associated with large block sizes. Specifically, we observe significant performance gains, with the progressive approach outperforming the direct baseline by 6.2 points on AIME24 and 4.8 points on Math500.

Table 3. Ablation on block size expansion strategies.

Strategy	AIME24	Math500
Direct Expansion	30.4	76.8
Progressive Expansion	36.3	81.6

6.3. Ablation on Think Coarse Critic Fine paradigm

We conduct an ablation study on the block size used in the thinking stage and the critic stage of the Think Coarse Critic Fine paradigm in Table 4. We find that using a smaller block size in the critic stage leads to a substantial performance improvement compared to a larger block size, while incurring only a minor efficiency loss. Using a small block size throughout the entire decoding process (i.e., $B = 1$) achieves the best performance, whereas using a large block size yields the highest decoding efficiency. The Think Coarse Critic Fine paradigm effectively combines the strengths of both settings, achieving a more favorable speed-effectiveness trade-off.

Table 4. Ablation on TCCF paradigm with different block sizes

Method	B_{think}	B_{critic}	Math500		AIME24	
			TPF	Acc	TPF	Acc
Dynamic Confidence	1	1	1.00	86.6	1.00	51.7
Dynamic Confidence	16	1	2.10	84.0	2.77	47.1
Dynamic Confidence	16	16	2.59	82.6	3.75	39.2
BACD	1	1	1.00	86.4	1.00	54.6
BACD	16	1	2.33	84.6	3.04	42.9
BACD	16	16	3.05	81.4	4.18	40.4

7. Related Work

7.1. Test Time Scaling and Efficient Reasoning

The success of OpenAI’s o1 introduced a new scaling paradigm, test-time compute scaling, which improves performance through increasing inference computation (OpenAI et al., 2024). However, while test-time scaling enhances reasoning capabilities, it inevitably leads to increasingly lengthy reasoning trajectories. Chen et al. (2025) reveals the “overthinking” phenomenon, showing that LRM s generate significantly more tokens than conventional LLMs on simple arithmetic tasks. To address this computational burden, existing research primarily focuses on reducing the number of tokens required for reasoning. Aggarwal & Welleck (2025) proposed length-controlled policy optimization, providing precise control over the length of the reasoning trajectories during generation. Similarly, Hao et al. (2024); Liu et al. (2025); Fang et al. (2025); Arora & Zanette (2025); Zhang et al. (2025) focused on fine-tuning models to think efficiently according to task complexity. In contrast to these approaches, diffusion language models (dLLMs), with their parallel decoding capabilities and bidirectional mechanisms, present a another promising direction to overcome these limitations and achieve more efficient reasoning inference.

7.2. Diffusion Language Models

Diffusion Language Models (DLMs) (Nie et al., 2025; Ye et al., 2025b; Austin et al., 2023; Sahoo et al., 2024) present

a promising alternative to the purely sequential generation of autoregressive models. By enabling the parallel generation of multiple tokens at each step, they offer a pathway toward significant inference acceleration. However, due to bidirectional attention mechanisms, DLMs typically lack support for exact KV caching. Block diffusion (Arriola et al., 2025) attempts to mitigate this issue by interpolating between discrete diffusion and autoregressive models. Recent works (Gong et al., 2025a; Ye et al., 2025b; Wu et al., 2025b; Cheng et al., 2025) leverage the efficiency of AR pre-training by initially training a standard LLM and subsequently adapting it to a diffusion-based objective. Building on this, Wang et al. (2025); Zhu et al. (2025c) incorporate Reinforcement Learning (RL) on top of architectures like SDAR (Cheng et al., 2025) to further enhance reasoning capabilities.

Block Diffusion Language Models (DLMs) have attracted increasing attention due to their potential for parallel generation. However, prior work has identified an inherent trade-off between parallelizability and generation quality. For Masked Diffusion Language Models, several efficient sampling algorithms have been proposed, including Entropy-Bounded Unmasking (Ben-Hamu et al., 2025), WINO (Hong et al., 2025), and Saber (Dong et al., 2025). In contrast, existing block diffusion models typically adopt static sampling strategies, such as fixing the number of tokens generated per step or applying a constant confidence threshold throughout decoding. Empirical results from open-source models such as SDAR (Cheng et al., 2025) and LLaDA 2 (Bie et al., 2025) suggest that high generation quality is often attained only when the decoding process approaches a near-autoregressive regime, i.e., generating approximately one token per step, thereby substantially diminishing the practical speed benefits of block-wise decoding.

8. Conclusion

In this paper, we propose a unified test-time scaling framework for Block Diffusion Language Models (BDLMs) that improves both reasoning quality and inference efficiency in long Chain-of-Thought reasoning. By introducing adaptivity in both decoding and block-wise generation, our framework effectively balances efficiency and reasoning quality under test-time scaling. In particular, Bounded Adaptive Confidence Decoding adapts the denoising process to model confidence, while Think Coarse, Critic Fine allocates different block sizes across different reasoning stages. Extensive experiments demonstrate that our framework significantly accelerates inference while improving performance on complex reasoning benchmarks. Overall, this work advances block diffusion language models for test-time scaling and provides a foundation for future research on block diffusion reasoning models.

Impact Statement

This work advances block diffusion language models by enabling adaptive test-time scaling, improving both efficiency and reasoning performance on complex tasks. Our methods focus on improving model inference and do not introduce direct ethical risks.

References

Aggarwal, P. and Welleck, S. L1: Controlling how long a reasoning model thinks with reinforcement learning, 2025. URL <https://arxiv.org/abs/2503.04697>.

AMC. American mathematics competition - amc. In *American Mathematics Competition - AMC*, 2023. URL <https://maa.org/student-programs/amc/>.

Arora, D. and Zanette, A. Training language models to reason efficiently, 2025. URL <https://arxiv.org/abs/2502.04463>.

Arriola, M., Gokaslan, A., Chiu, J. T., Yang, Z., Qi, Z., Han, J., Sahoo, S. S., and Kuleshov, V. Block diffusion: Interpolating between autoregressive and diffusion language models. *arXiv preprint arXiv:2503.09573*, 2025.

Austin, J., Johnson, D. D., Ho, J., Tarlow, D., and van den Berg, R. Structured denoising diffusion models in discrete state-spaces, 2023. URL <https://arxiv.org/abs/2107.03006>.

Ben-Hamu, H., Gat, I., Severo, D., Nolte, N., and Karrer, B. Accelerated sampling from masked diffusion models via entropy bounded unmasking, 2025. URL <https://arxiv.org/abs/2505.24857>.

Bie, T., Cao, M., Chen, K., Du, L., Gong, M., Gong, Z., Gu, Y., Hu, J., Huang, Z., Lan, Z., et al. Llada2.0: Scaling up diffusion language models to 100b. *arXiv preprint arXiv:2512.15745*, 2025.

Chen, X., Xu, J., Liang, T., He, Z., Pang, J., Yu, D., Song, L., Liu, Q., Zhou, M., Zhang, Z., Wang, R., Tu, Z., Mi, H., and Yu, D. Do not think that much for 2+3=? on the overthinking of o1-like llms, 2025. URL <https://arxiv.org/abs/2412.21187>.

Cheng, S., Bian, Y., Liu, D., Zhang, L., Yao, Q., Tian, Z., Wang, W., Guo, Q., Chen, K., Qi, B., et al. Sdar: A synergistic diffusion-autoregression paradigm for scalable sequence generation. *arXiv preprint arXiv:2510.06303*, 2025.

Dong, Y., Ma, Z., Jiang, X., Fan, Z., Qian, J., Li, Y., Xiao, J., Jin, Z., Cao, R., Li, B., Huang, F., Li, Y., and Li, G. Saber: An efficient sampling with adaptive acceleration and backtracking enhanced remasking for diffusion language model, 2025. URL <https://arxiv.org/abs/2510.18165>.

Fang, G., Ma, X., and Wang, X. Thinkless: Llm learns when to think, 2025. URL <https://arxiv.org/abs/2505.13379>.

Gemini. Gemini diffusion, our state-of-the-art, experimental text diffusion model, 2025. URL <https://deepmind.google/models/gemini-diffusion/>.

Gong, S., Agarwal, S., Zhang, Y., Ye, J., Zheng, L., Li, M., An, C., Zhao, P., Bi, W., Han, J., Peng, H., and Kong, L. Scaling diffusion language models via adaptation from autoregressive models, 2025a. URL <https://arxiv.org/abs/2410.17891>.

Gong, S., Zhang, R., Zheng, H., Gu, J., Jaitly, N., Kong, L., and Zhang, Y. Diffucoder: Understanding and improving masked diffusion models for code generation, 2025b. URL <https://arxiv.org/abs/2506.20639>.

Hao, S., Sukhbaatar, S., Su, D., Li, X., Hu, Z., Weston, J., and Tian, Y. Training large language models to reason in a continuous latent space, 2024. URL <https://arxiv.org/abs/2412.06769>.

Hendrycks, D., Burns, C., Kadavath, S., Arora, A., Basart, S., Tang, E., Song, D., and Steinhardt, J. Measuring mathematical problem solving with the math dataset. *arXiv preprint arXiv:2103.03874*, 2021.

Hong, F., Yu, G., Ye, Y., Huang, H., Zheng, H., Zhang, Y., Wang, Y., and Yao, J. Wide-in, narrow-out: Revokable decoding for efficient and effective dllms, 2025. URL <https://arxiv.org/abs/2507.18578>.

Jain, N., Han, K., Gu, A., Li, W.-D., Yan, F., Zhang, T., Wang, S., Solar-Lezama, A., Sen, K., and Stoica, I. Livecodebench: Holistic and contamination free evaluation of large language models for code, 2024. URL <https://arxiv.org/abs/2403.07974>.

Langley, P. Crafting papers on machine learning. In Langley, P. (ed.), *Proceedings of the 17th International Conference on Machine Learning (ICML 2000)*, pp. 1207–1216, Stanford, CA, 2000. Morgan Kaufmann.

Liu, W., Zhou, R., Deng, Y., Huang, Y., Liu, J., Deng, Y., Zhang, Y., and He, J. Learn to reason efficiently with adaptive length-based reward shaping, 2025. URL <https://arxiv.org/abs/2505.15612>.

MAA. American invitational mathematics examination-aime 2024, 2024. URL <https://huggingface.co/datasets/math-ai/aime24>.

MAA. American invitational mathematics examination-aime 2025, 2025. URL <https://huggingface.co/datasets/math-ai/aime25>.

Nie, S., Zhu, F., Du, C., Pang, T., Liu, Q., Zeng, G., Lin, M., and Li, C. Scaling up masked diffusion models on text. *arXiv preprint arXiv:2410.18514*, 2024.

Nie, S., Zhu, F., You, Z., Zhang, X., Ou, J., Hu, J., ZHOU, J., Lin, Y., Wen, J.-R., and Li, C. Large language diffusion models. In *ICLR 2025 Workshop on Deep Generative Model in Machine Learning: Theory, Principle and Efficiency*, 2025.

OpenAI, :, Jaech, A., Kalai, A., Lerer, A., Richardson, A., El-Kishky, A., Low, A., Helyar, A., Madry, A., Beutel, A., Carney, A., Iftimie, A., Karpenko, A., Passos, A. T., Neitz, A., Prokofiev, A., Wei, A., Tam, A., Bennett, A., Kumar, A., Saraiva, A., Vallone, A., Duberstein, A., Kondrich, A., Mishchenko, A., Applebaum, A., Jiang, A., Nair, A., Zoph, B., Ghorbani, B., Rossen, B., Sokolowsky, B., Barak, B., McGrew, B., Minaev, B., Hao, B., Baker, B., Houghton, B., McKinzie, B., Eastman, B., Lugaressi, C., Bassin, C., Hudson, C., Li, C. M., de Bourcy, C., Voss, C., Shen, C., Zhang, C., Koch, C., Orsinger, C., Hesse, C., Fischer, C., Chan, C., Roberts, D., Kappler, D., Levy, D., Selsam, D., Dohan, D., Farhi, D., Mely, D., Robinson, D., Tsipras, D., Li, D., Oprica, D., Freeman, E., Zhang, E., Wong, E., Proehl, E., Cheung, E., Mitchell, E., Wallace, E., Ritter, E., Mays, E., Wang, F., Such, F. P., Raso, F., Leoni, F., Tsimpourlas, F., Song, F., von Lohmann, F., Sulit, F., Salmon, G., Parascandolo, G., Chabot, G., Zhao, G., Brockman, G., Leclerc, G., Salman, H., Bao, H., Sheng, H., Andrin, H., Bagherinezhad, H., Ren, H., Lightman, H., Chung, H. W., Kivlichan, I., O'Connell, I., Osband, I., Gilaberte, I. C., Akkaya, I., Kostrikov, I., Sutskever, I., Kofman, I., Pachocki, J., Lennon, J., Wei, J., Harb, J., Twore, J., Feng, J., Yu, J., Weng, J., Tang, J., Yu, J., Candela, J. Q., Palermo, J., Parish, J., Heidecke, J., Hallman, J., Rizzo, J., Gordon, J., Uesato, J., Ward, J., Huizinga, J., Wang, J., Chen, K., Xiao, K., Singhal, K., Nguyen, K., Cobbe, K., Shi, K., Wood, K., Rimbach, K., Gu-Lemberg, K., Liu, K., Lu, K., Stone, K., Yu, K., Ahmad, L., Yang, L., Liu, L., Maksin, L., Ho, L., Fedus, L., Weng, L., Li, L., McCallum, L., Held, L., Kuhn, L., Kondraciuk, L., Kaiser, L., Metz, L., Boyd, M., Trebacz, M., Joglekar, M., Chen, M., Tintor, M., Meyer, M., Jones, M., Kaufer, M., Schwarzer, M., Shah, M., Yatbaz, M., Guan, M. Y., Xu, M., Yan, M., Glaese, M., Chen, M., Lampe, M., Malek, M., Wang, M., Fradin, M., McClay, M., Pavlov, M., Wang, M., Wang, M., Murati, M., Bavarian, M., Rohaninejad, M., McAleese, N., Chowdhury, N., Chowdhury, N., Ryder, N., Tezak, N., Brown, N., Nachum, O., Boiko, O., Murk, O., Watkins, O., Chao, P., Ashbourne, P., Izmailov, P., Zhokhov, P., Dias, R., Arora, R., Lin, R., Lopes, R. G., Gaon, R., Miyara, R., Leike, R., Hwang, R., Garg, R., Brown, R., James, R., Shu, R., Cheu, R., Greene, R., Jain, S., Altman, S., Toizer, S., Toyer, S., Miserendino, S., Agarwal, S., Hernandez, S., Baker, S., McKinney, S., Yan, S., Zhao, S., Hu, S., Santurkar, S., Chaudhuri, S. R., Zhang, S., Fu, S., Papay, S., Lin, S., Balaji, S., Sanjeev, S., Sidor, S., Broda, T., Clark, A., Wang, T., Gordon, T., Sanders, T., Patwardhan, T., Sottiaux, T., Degry, T., Dimson, T., Zheng, T., Garipov, T., Stasi, T., Bansal, T., Creech, T., Peterson, T., Eloundou, T., Qi, V., Kosaraju, V., Monaco, V., Pong, V., Fomenko, V., Zheng, W., Zhou, W., McCabe, W., Zaremba, W., Dubois, Y., Lu, Y., Chen, Y., Cha, Y., Bai, Y., He, Y., Zhang, Y., Wang, Y., Shao, Z., and Li, Z. Openai 01 system card, 2024. URL <https://arxiv.org/abs/2412.16720>.

Rein, D., Hou, B. L., Stickland, A. C., Petty, J., Pang, R. Y., Dirani, J., Michael, J., and Bowman, S. R. Gpqa: A graduate-level google-proof qa benchmark, 2023. URL <https://arxiv.org/abs/2311.12022>.

Sahoo, S. S., Arriola, M., Schiff, Y., Gokaslan, A., Marroquin, E., Chiu, J. T., Rush, A., and Kuleshov, V. Simple and effective masked diffusion language models, 2024. URL <https://arxiv.org/abs/2406.07524>.

Shao, C., Ren, S., Xu, F., and Li, Y. Diffuse thinking: Exploring diffusion language models as efficient thought proposers for reasoning. *arXiv preprint arXiv:2510.27469*, 2025.

Wang, Y., Yang, L., Li, B., Tian, Y., Shen, K., and Wang, M. Revolutionizing reinforcement learning framework for diffusion large language models. *arXiv preprint arXiv:2509.06949*, 2025.

Wu, C., Zhang, H., Xue, S., Diao, S., Fu, Y., Liu, Z., Molchanov, P., Luo, P., Han, S., and Xie, E. Fast-dllm v2: Efficient block-diffusion llm. *arXiv preprint arXiv:2509.26328*, 2025a.

Wu, C., Zhang, H., Xue, S., Diao, S., Fu, Y., Liu, Z., Molchanov, P., Luo, P., Han, S., and Xie, E. Fast-dllm v2: Efficient block-diffusion llm, 2025b. URL <https://arxiv.org/abs/2509.26328>.

Wu, C., Zhang, H., Xue, S., Liu, Z., Diao, S., Zhu, L., Luo, P., Han, S., and Xie, E. Fast-dllm: Training-free acceleration of diffusion llm by enabling kv cache and parallel decoding. *arXiv preprint arXiv:2505.22618*, 2025c.

Wu, C., Zhang, H., Xue, S., Liu, Z., Diao, S., Zhu, L., Luo, P., Han, S., and Xie, E. Fast-dllm: Training-free acceleration of diffusion llm by enabling kv cache and parallel decoding, 2025d. URL <https://arxiv.org/abs/2505.22618>.

Ye, J., Gao, J., Gong, S., Zheng, L., Jiang, X., Li, Z., and Kong, L. Beyond autoregression: Discrete diffusion for complex reasoning and planning, 2025a. URL <https://arxiv.org/abs/2410.14157>.

Ye, J., Xie, Z., Zheng, L., Gao, J., Wu, Z., Jiang, X., Li, Z., and Kong, L. Dream 7b: Diffusion large language models. *arXiv preprint arXiv:2508.15487*, 2025b.

Zhang, J., Lin, N., Hou, L., Feng, L., and Li, J. Adapthink: Reasoning models can learn when to think, 2025. URL <https://arxiv.org/abs/2505.13417>.

Zhu, F., Wang, R., Nie, S., Zhang, X., Wu, C., Hu, J., Zhou, J., Chen, J., Lin, Y., Wen, J.-R., and Li, C. Llada 1.5: Variance-reduced preference optimization for large language diffusion models, 2025a. URL <https://arxiv.org/abs/2505.19223>.

Zhu, F., You, Z., Xing, Y., Huang, Z., Liu, L., Zhuang, Y., Lu, G., Wang, K., Wang, X., Wei, L., Guo, H., Hu, J., Ye, W., Chen, T., Li, C., Tang, C., Feng, H., Hu, J., Zhou, J., Zhang, X., Lan, Z., Zhao, J., Zheng, D., Li, C., Li, J., and Wen, J.-R. Llada-moe: A sparse moe diffusion language model, 2025b. URL <https://arxiv.org/abs/2509.24389>.

Zhu, Y., Wan, J., Liu, X., He, S., Wang, Q., Guo, X., Liang, T., Huang, Z., He, Z., and Qiu, X. Dirl: An efficient post-training framework for diffusion language models. *arXiv preprint arXiv:2512.22234*, 2025c.

A. Comparison between AR and Block Diffusion Base Models

For fair comparison, we train an autoregressive baseline model from Qwen3-8B-base following an identical training recipe. Table 5 compares our base model with Qwen3-8B-base[†].

Table 5. Performance comparison of base models across different benchmarks.

Model	MMLU	CMMLU	GSM8k	Math500	HumanEval
Qwen3-8B-base [†]	76.32	77.06	85.30	44.32	57.93
TDAR-8B-Base ($B = 4$)	74.18	74.42	87.14	40.74	52.44

B. Implementation Details

B.1. Model Training Configuration

We transform Qwen3-8B-base into Block DLMs following the methodology of Cheng et al. (2025). Initially, we modify the generation mechanism through blockwise diffusion objective training ($B = 4$) on a 50B-token annealing corpus subset, yielding TDAR-8B-Base ($B = 4$).

Next, we conduct Supervised Fine-Tuning (SFT) on 3B long Chain-of-Thought (CoT) datasets employing our progressive block-size expansion approach. Starting from block size 4, we gradually increase the training block size to 64 while maintaining consistent training configurations. Each stage undergoes 3 training epochs. Detailed training specifications are presented in Table 6.

Table 6. Training configuration details for each stage.

Stage	Tokens	Epochs	Learning Rate	Batch Size
CPT	50B	1	1e-4	1024
SFT	3B	3	3e-5	128

B.2. Inference Configuration

We utilize LMDeploy² as our inference engine, which provides efficient support for both autoregressive and block diffusion decoding. All experiments are conducted on NVIDIA H200 GPUs.

We configure the maximum generation length to 30,000 tokens for SDAR-8B-Chat, DiRL-8B-Instruct, all TraDo-8B variants and our TDAR-8B-thinking model, which is sufficient for long Chain-of-Thought reasoning trajectories. We use a temperature of 1.0 to encourage diverse responses, while top-p and top-k sampling are not employed in our main experiments.

C. Detailed Usage of TCCF Paradigm

The Think Coarse, Critic Fine (TCCF) paradigm implements a two-stage reasoning process that adaptively adjusts block sizes according to the functional roles of different reasoning segments. The paradigm exploits the observation that early-stage exploratory reasoning can tolerate coarse-grained generation, while later-stage refinement and verification require fine-grained precision. Algorithm 2 presents the complete TCCF inference procedure.

Stage 1: Coarse Thinking ($B_{think} = 16$): In the first stage, the model performs exploratory reasoning with a large block size to efficiently generate the initial reasoning trajectory. The model processes the input prompt p and generates reasoning content until it reaches the designated thinking boundary marker $</\text{think}>$. During this stage, the model rapidly explores the solution space, proposes potential approaches, and conducts preliminary analysis. The large block size ($B_{think} = 16$) enables efficient parallel decoding, significantly accelerating the exploration process.

Transition Mechanism: Once the model completes the thinking stage, the system automatically replaces this marker with

²<https://github.com/InternLM/lmdeploy>

a transition prompt: “Let’s check if there are any mistakes and give the final answer.” This prompt serves as an explicit instruction to shift the model’s focus from exploration to verification and refinement.

Stage 2: Fine Critic ($B_{critic} = 1$): In the second stage, the model switches to a smaller block size ($B_{critic} = 1$, equivalent to autoregressive decoding) to perform careful verification and refinement. The model reviews the reasoning generated in Stage 1, identifies potential errors, corrects mistakes, and produces the final answer with high reliability. The fine-grained decoding ensures precision in the critical refinement phase while maintaining computational efficiency overall, since Stage 2 typically generates significantly fewer tokens than Stage 1.

Algorithm 2: Think Coarse, Critic Fine (TCCF) Inference

Require: Input prompt p , model θ , thinking block size B_{think} , critic block size B_{critic} , transition prompt p_{trans}

Ensure: Final response y

```

1: // Stage 1: Coarse Thinking
2: Initialize reasoning trajectory  $r \leftarrow$  empty string
3: Set current block size  $B \leftarrow B_{think}$ 
4: while  $r$  does not contain  $</\text{think}>$  do
5:   Generate next block:  $r_{new} \sim p_{\theta}(\cdot | p, r; B)$ 
6:   Append to trajectory:  $r \leftarrow r + r_{new}$ 
7: end while
8: // Transition: Replace marker with refinement prompt
9:  $r \leftarrow$  replace( $</\text{think}>$  in  $r$  with  $p_{trans}$ )
10: // Stage 2: Fine Critic
11: Initialize final response  $y \leftarrow r$ 
12: Set current block size  $B \leftarrow B_{critic}$ 
13: while not end-of-sequence do
14:   Generate next block:  $y_{new} \sim p_{\theta}(\cdot | p, y; B)$ 
15:   Append to response:  $y \leftarrow y + y_{new}$ 
16:   if  $y$  contains end-of-sequence token then
17:     break
18:   end if
19: end while
20: return  $y$ 

```

Prompt 1: Transition prompt used in TCCF

Let’s check if there are any mistakes and give the final answer.

Figure 8. Transition prompt used in TCCF paradigm to shift from coarse thinking ($B_{think} = 16$) to fine critic stage ($B_{critic} = 1$). This prompt is automatically inserted at the position where $</\text{think}>$ marker appears in the Stage 1 output.

Discussion on marker for boundary detection: The TCCF paradigm is highly flexible and generalizable. Depending on the task requirements or model characteristics, the transition mechanism can be adapted using alternative prompt formulations (e.g., “Review the steps above” or “Summarize the solution”), or by employing different structural markers. Our implementation provides a foundational framework for test-time scaling in Block DLMs, offering a broad design space for future exploration in efficient and reliable long-context reasoning.

D. Efficiency Analysis on Industrial Inference Engines

To evaluate the practical deployment potential of our method in real-world industrial scenarios, we conducted a comprehensive efficiency test comparing our **BACD** decoding strategy against the standard Dynamic Confidence baseline.

We utilized the TDAR-8B-thinking model for all tests and measured the decoding throughput in **tokens per second (TPS)** across a range of batch sizes ($BS \in \{1, 4, 8, 16, 32\}$) on a single NVIDIA H200 GPU. As illustrated in Figure 9, BACD consistently outperforms the baseline across all tested batch sizes.

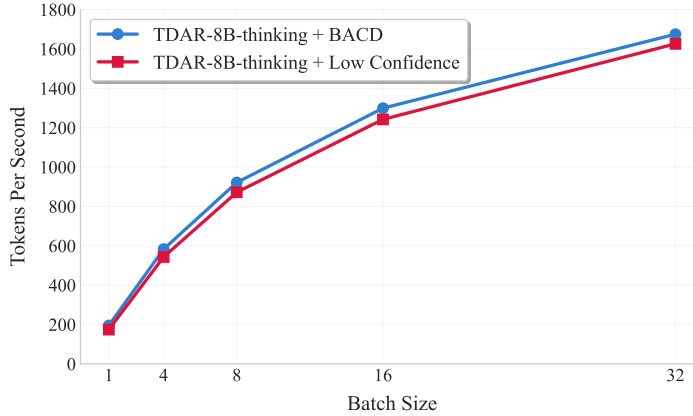


Figure 9. Decoding efficiency on TDAR-8B-thinking, ranging from single-stream ($BS = 1$) to high-throughput ($BS = 32$) settings.

In addition, we observe clear throughput scaling behavior as batch size increases. At the single-stream setting ($BS = 1$), BACD achieves 195 TPS. As batch size scales up, throughput increases substantially. Under the high-throughput scenario ($BS = 32$), BACD delivers 1675 TPS, demonstrating its capability to handle large-scale concurrent inference requests efficiently.

E. Comparison with other Decoding Methods

To comprehensively evaluate the effectiveness of our proposed BACD method, we compare it against several established decoding strategies for Block Diffusion Language Models. We consider Confidence Static decoding, which uses a fixed number of denoising steps equal to the block size ($N = B$), representing the lowest efficiency ($TPF = 1$). Confidence Dynamic decoding dynamically terminates generation based on a single confidence threshold, offering a baseline for adaptive approaches.

Most notably, we compare against Entropy-bounded sampling (Ben-Hamu et al., 2025). The Entropy-bounded sampler addresses the joint dependence error that arises when multiple tokens are unmasked simultaneously by computing a cumulative entropy bound: at each step, it sorts masked tokens by an error proxy (e.g., entropy or confidence) and selects the largest subset of tokens U such that $\sum_{l \in U} H(p_\theta(x^l | x^{\bar{M}})) - \max_{l \in U} H(p_\theta(x^l | x^{\bar{M}})) \leq \gamma$, where γ is a hyperparameter controlling the accuracy-efficiency trade-off. We used confidence as error proxy in our experiments.

Table 7 presents detailed comparison results on Math500 and AIME24 benchmarks across different γ configurations ($\gamma \in \{0.3, 0.5, 0.7\}$) for the Entropy-bounded method. On Math500, even at the most aggressive setting ($\gamma = 0.7$), Entropy-bounded only achieves a TPF of 1.86, barely surpassing our BACD method's 1.88, yet suffers a catastrophic accuracy drop to 77.6%. At more conservative settings that preserve accuracy ($\gamma = 0.3$, achieving 81.4% accuracy), the method's TPF of 1.63 provides minimal acceleration over single-token decoding. In contrast, BACD achieves a TPF of 1.88 while maintaining 83.4% accuracy, effectively matching the Static baseline's quality (83.8%) with nearly 2x speedup.

On the more challenging AIME24 benchmark, while Entropy-bounded ($\gamma = 0.3$) attains the highest accuracy of 44.58%, it does so at a TPF of merely 1.53. As γ increases to enable faster decoding, accuracy deteriorates rapidly: at $\gamma = 0.7$, accuracy plummets to 35.83% despite only reaching a TPF of 1.64. BACD, on the other hand, achieves a remarkable TPF of 5.07, more than 3x faster than any Entropy-bounded configuration while maintaining competitive accuracy at 36.25%. This demonstrates that BACD successfully unlocks a high-efficiency operating regime that Entropy-bounded methods fundamentally fail to access.

F. Case Study

Figure 10 presents a detailed case study demonstrating why the TCCF paradigm is crucial for complex reasoning tasks. The problem asks for the least possible sum of distinct positive integers with product 84, which requires searching through multiple factor combinations.

Table 7. Comparison of different decoding methods on Math500 and AIME24. BACD achieves the best efficiency-accuracy trade-off.

Method	Math500		AIME24	
	TPF	Acc	TPF	Acc
Confidence Static	1.00	83.80	1.00	39.58
Confidence Dynamic	1.62	81.60	4.47	34.58
Entropy-bounded ($\gamma = 0.3$)	1.63	81.40	1.53	44.58
Entropy-bounded ($\gamma = 0.5$)	1.77	81.00	1.59	43.75
Entropy-bounded ($\gamma = 0.7$)	1.86	77.60	1.64	35.83
BACD (Ours)	1.88	83.40	5.07	36.25

Stage 1: Efficient Exploration via Coarse Thinking ($B = 16$). In this phase, the model acts as a rapid explorer. By using a large block size, it can quickly traverse the reasoning path and identify high-probability solutions. As shown in the case, the model correctly identifies the factorization of 84 and proposes several valid sets, arriving at a suboptimal answer of 15. Although the coarse granularity ($B = 16$) accelerates the generation of the reasoning chain, it inherently carries a trade-off in precision, leading the model to overlook the optimal combination $\{3, 4, 7\}$ in the vast search space. This stage provides the necessary *breadth* of reasoning without consuming excessive computational time.

Stage 2: Precision Correction via Fine Critic ($B = 1$). The transition prompt (“Let’s check...”) triggers a mode switch, acting as a verifier. By switching to the finest granularity ($B = 1$), the model allocates its full computational capacity to scrutinize the previous conclusion. In this high-precision mode, the model successfully detects the oversight from the coarse stage and discovers the subtle combination $\{3, 4, 7\}$ (sum=14).

Effectiveness Analysis: This case illustrates the core advantage of TCCF. It decouples reasoning generation from answer verification. Pure coarse decoding ($B = 16$) is fast but prone to detail errors (finding 15 instead of 14), while pure fine decoding ($B = 1$) is accurate but computationally expensive. TCCF using the first stage to efficiently narrow down the solution space and the second stage to ensure the final answer is precise. This coarse-to-fine mechanism allows the model to correct its own hallucinations or oversights, directly contributing to the accuracy improvements observed in our benchmarks.

Prompt 2: Model Output

Problem: The product of a set of distinct positive integers is 84. What is the least possible sum of these integers?

Stage1 Output:

<think>

We need to find a set of distinct positive integers (i.e., the integers are all different) whose product is 84, and we want to minimize the sum of the integers.

First, note that factorization of $84 = 2^2 * 3 * 7 \dots$

Potential sets:

- Single integer: 84 sum = 84.
- Two numbers: distinct positive integers a, b, $a*b=84 \dots$ minimal sum among two numbers without 1 is 19 (7+12).
- Three numbers: $a*b*c=84$, distinct $>1 \dots$ We found such: 2,3,14 sum=19; 2,4,21 sum=27; 2,6,14 sum=22; 2,7,12 sum=21; 3,4,14 sum=21. So minimal sum among three numbers is 19.
- Four numbers: ... we could have 4,3,7,1 product = $4*3*7*1 = 84 \dots$ Sum = $4+3+7+1 = 15$.

Thus the minimal sum among sets of size 4 is 15.

Now we need to produce final answer.

Let's check if there are any mistakes and give the final answer.

Stage2 Output:

Let me pause and think about this more carefully... But we need to also consider if there is any other set with sum 14? Let's see if there's any set of size >1 with sum 14? The set 1,3,4,7 sum = 15. No, sum 14 would require 1,3,4,6? Product = 72 not 84...

But I should also consider whether the problem intends the set to contain at least two integers... However, the set with sum 14 includes 3 numbers, all distinct >0 , product 84. So if we allow any cardinality ≥ 2 , the minimum sum is 14. But we need to verify if there is a set of size 2 with sum less than 14. The minimum sum among pairs not including 1 is 19. So no. So if cardinality ≥ 2 , the answer is 14. But we have a set of size 3 and sum 14. So answer would be 14, not 15.

But we need to see what the problem expects... Actually $14 < 15$. But we found a set of three numbers with sum 14 (3+4+7). So sum 14 is less. So the minimal sum must be ≤ 14 . But we found a set 3,4,7 sum = 14, product = 84. So sum 14 is possible.

Wait we need to double-check: Are there any sets of size ≥ 4 with sum < 14 ? Possibly 1,3,4,7 sum = 15 which is higher than 14. So minimal sum is 14...

But earlier we thought of including 1 to reduce sum further. The minimal sum is 14 from 3,4,7. So answer is 14.

Thus final answer: 14. Let's produce final answer accordingly.

</think>

Final Answer:

The prime factorisation of $84 = 2^2 \cdot 3 \cdot 7$. Considering all possible sets of distinct positive integers with product 84:

- One integer: 84 \rightarrow sum = 84
- Two integers: minimal sum = $7+12 = 19$
- Three integers: minimal sum = $3+4+7 = 14$ (set 3,4,7)
- Four integers: must include 1, minimal sum = $1+3+4+7 = 15$
- Five or more integers: impossible

The smallest achievable sum is 14.

Figure 10. Case study of a representative problem from the Math500 benchmark.